



ISTITUTO NAZIONALE DI RICERCA METROLOGICA Repository Istituzionale

Gene editing reverses arrhythmia susceptibility in humanized PLN-R14del mice: modelling a European cardiomyopathy with global impact

Original

Gene editing reverses arrhythmia susceptibility in humanized PLN-R14del mice: modelling a European cardiomyopathy with global impact / Dave, J., Raad, N., Mittal, N., Zhang, L.u., Fagnoli, A., Gyun Oh, J., Elisabetta Savoia, M., Hansen, J., Fava, M., Yin, X., Theofilatos, K., Ceholski, D., Kohlbrenner, E., Jeong, D., Wills, L., Nonnenmacher, M., Haghghi, K., D Costa, K., C Turnbull, I., Mayr, M., et al.. - In: CARDIOVASCULAR RESEARCH. - ISSN 1755-3245. - 118:15(2022). [10.1093/cvr/cvac021]

Availability:

This version is available at: 11696/85259 since: 2025-02-19T08:09:06Z

Publisher:

Oxford University Press

Published

DOI:10.1093/cvr/cvac021

Terms of use:

This article is made available under terms and conditions as specified in the corresponding bibliographic description in the repository

Publisher copyright

(Article begins on next page)

Gene editing reverses arrhythmia susceptibility in humanized PLN-R14del mice: modelling a European cardiomyopathy with global impact

Jaydev Dave ¹, Nour Raad¹, Nishka Mittal¹, Lu Zhang², Anthony Fargnoli¹, Jae Gyun Oh¹, Maria Elisabetta Savoia¹, Jens Hansen³, Marika Fava¹, Xiaoke Yin ⁴, Konstantinos Theofilatos ⁴, Delaine Ceholski ¹, Erik Kohlbrenner¹, Dongtak Jeong⁵, Lauren Wills ¹, Mathieu Nonnenmacher¹, Kobra Haghghi ⁶, Kevin D. Costa ¹, Irene C. Turnbull¹, Manuel Mayr ^{1,4}, Chen-Leng Cai ², Evangelia G. Kranias⁶, Fadi G. Akar ¹, Roger J. Hajjar⁷, and Francesca Stillitano ^{1*}

¹Cardiovascular Research Center, Icahn School of Medicine at Mount Sinai, New York, NY, USA; ²Department of Pediatrics, Riley Heart Research Center, Herman B Wells Center for Pediatric Research, Indiana University School of Medicine, Indianapolis, IN, USA; ³Department of Pharmacological Sciences and Institute for Systems Biomedicine, Icahn School of Medicine at Mount Sinai, New York, NY, USA; ⁴King's British Heart Foundation Centre, King's College London, London, UK; ⁵Department of Molecular & Life Science, College of Science and Convergence Technology, Hanyang University-ERICA, Ansan-si, South Korea; ⁶Department of Pharmacology and Systems Physiology, University of Cincinnati College of Medicine, Cincinnati, OH, USA; and ⁷Phospholamban Foundation, Amsterdam, Netherlands

Received 9 June 2020; editorial decision 8 February 2022; accepted 18 February 2022; online publish-ahead-of-print 22 February 2022

Time for primary review: 56 days

See the editorial comment for this article 'Gene editing for cardiomyopathy takes a step forward', by Mauro Giacca, <https://doi.org/10.1093/cvr/cvac164>.

Aims

A mutation in the phospholamban (PLN) gene, leading to deletion of Arg14 (R14del), has been associated with malignant arrhythmias and ventricular dilation. Identifying pre-symptomatic carriers with vulnerable myocardium is crucial because arrhythmia can result in sudden cardiac death, especially in young adults with PLN-R14del mutation. This study aimed at assessing the efficiency and efficacy of *in vivo* genome editing, using CRISPR/Cas9 and a cardiotropic adeno-associated virus-9 (AAV9), in improving cardiac function in young adult mice expressing the human PLN-R14del.

Methods and results

Humanized mice were generated expressing human wild-type (hPLN-WT) or mutant (hPLN-R14del) PLN in the heterozygous state, mimicking human carriers. Cardiac magnetic resonance imaging at 12 weeks of age showed bi-ventricular dilation and increased stroke volume in mutant vs. WT mice, with no deficit in ejection fraction or cardiac output. Challenge of *ex vivo* hearts with isoproterenol and rapid pacing unmasked higher propensity for sustained ventricular tachycardia (VT) in hPLN-R14del relative to hPLN-WT. Specifically, the VT threshold was significantly reduced (20.3 ± 1.2 Hz in hPLN-R14del vs. 25.7 ± 1.3 Hz in WT, $P < 0.01$) reflecting higher arrhythmia burden. To inactivate the R14del allele, mice were tail-vein-injected with AAV9.CRISPR/Cas9/gRNA or AAV9 empty capsid (controls). CRISPR-Cas9 efficiency was evaluated by droplet digital polymerase chain reaction and NGS-based amplicon sequencing. *In vivo* gene editing significantly reduced end-diastolic and stroke volumes in hPLN-R14del CRISPR-treated mice compared to controls. Susceptibility to VT was also reduced, as the VT threshold was significantly increased relative to controls (30.9 ± 2.3 Hz vs. 21.3 ± 1.5 Hz; $P < 0.01$).

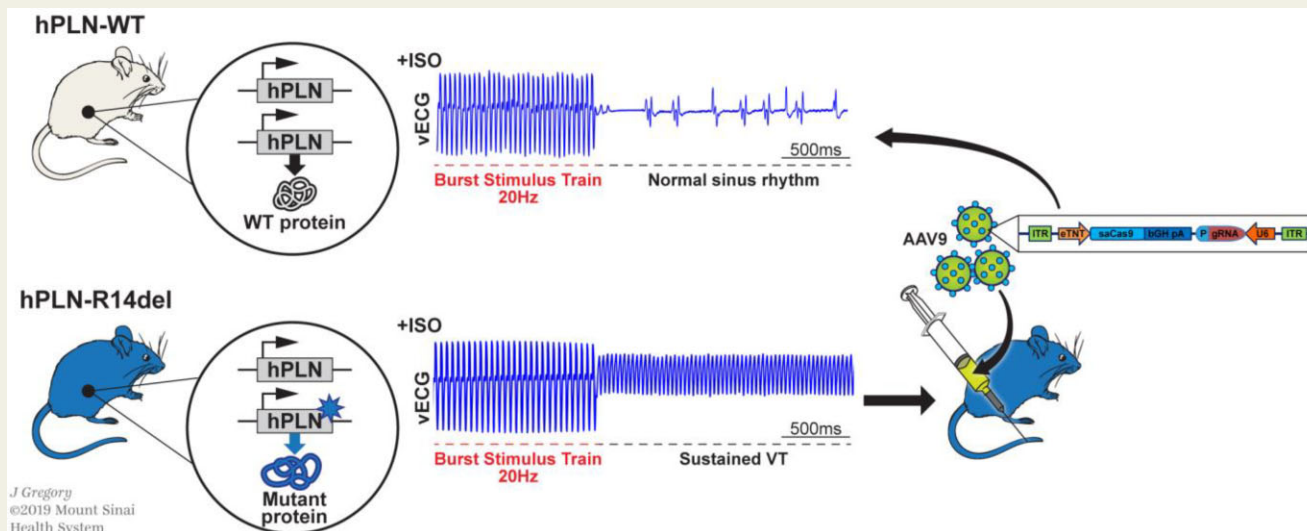
Conclusions

This study is the first to show that disruption of hPLN-R14del allele by AAV9-CRISPR/Cas9 improves cardiac function and reduces VT susceptibility in humanized PLN-R14del mice, offering preclinical evidence for translatable approaches to therapeutically suppress the arrhythmogenic phenotype in human patients with PLN-R14del disease.

*Corresponding author. Tel: +1 212 824 8907, E-mail: francesca.stillitano@mssm.edu

[‡]This manuscript was handled by a Consulting Editor, Professor Godfrey Smith.

Graphical Abstract



Keywords

Humanized mouse • Phospholamban R14del mutation • CRISPR/Cas9 • Ventricular tachycardia • Gene therapy

1. Introduction

Phospholamban (PLN) is a small integral protein of the sarcoplasmic reticulum (SR) membrane and a major regulator of the sarco/endoplasmic reticulum Ca-ATPase (SERCA2a) pump, and therefore, of excitation–contraction coupling and overall cardiac function. Mutations in the human *PLN* gene cause disruption of the delicate balance that governs PLN protein interaction with SERCA2a and have been linked to familial cardiomyopathy. The PLN-R14del mutation consists of a nucleotide triplet (AGA) deletion which results in the loss of a highly conserved amino acid, Arginine 14. The PLN-R14del mutation was first discovered in a large Greek family with clinical manifestations of both dilated cardiomyopathy (DCM) and arrhythmogenic cardiomyopathy (ACM).¹ In the Netherlands, a larger cohort of patients with ACM or DCM (12–15%) were subsequently identified as PLN-R14del carriers.^{2,3} The founder effect of this mutation is thought to have originated in the northern part of the Netherlands with all Dutch patients carrying the same haplotype, which is estimated to be between 575 and 825 years old.² The PLN-R14del mutation has also been identified in multiple families in other parts of Europe^{4,5} and North America.⁶ All the known carriers and patients alike are heterozygous for the mutation. The clinical phenotype associated with the PLN-R14del mutation is highly variable and includes phenotypic characteristics of ACM and DCM with pervasive malignant ventricular tachycardia (VT) that appears to be age-dependent and significantly increases the mortality rate of these patients.^{1,7,8} With variable penetrance, PLN-R14del disease manifestation remains unpredictable. However, most patients come to clinical attention in the fourth decade of life.³

Extensive epidemiological studies showed that many PLN-R14del carriers remain asymptomatic.⁹ Little is known regarding the triggers that could influence the clinical course of the disease in an individual carrier. Major efforts are underway to understand which genetic, molecular, or

exogenous factors could affect the appearance and progression of ventricular dysfunction, and the increased vulnerability to arrhythmias in heterozygous carriers. Special interest has been focused on SERCA2a–PLN interaction, but the mutated form of PLN may have effects beyond SR Ca-cycling impairment. Early studies in mouse models identified PLN-R14del as a strong inhibitor of SERCA2a, when overexpressed in the presence of wild-type (WT) PLN.¹ Subsequently, it was shown that the mutant protein mislocalized to the sarcolemma in the absence of endogenous WT PLN, and it activated the Na/K-ATPase.¹⁰ However, the underlying mechanisms by which genetic defects in Ca-cycling proteins (and specifically PLN) are linked to pathophysiology remain unclear, reflecting major discrepancies in phenotype between humans and mice.

More recent studies utilizing ‘humanized’ *in vitro* systems with either induced pluripotent stem cell derived-cardiomyocytes (iPSC-CMs) or three-dimensional engineered cardiac tissue (hECT) aimed to further address the functional role of this PLN mutation in the heart. iPSC-CMs derived from patients harbouring PLN-R14del mutation were shown to exhibit frequent episodes of irregular Ca²⁺ waves, electrical instability, abnormal cytoplasmic distribution of PLN and an increased expression of molecular markers associated with cardiac hypertrophy.¹¹ Using TALEN-mediated genome editing, R14del mutation was corrected in iPSCs and the derived CMs exhibited normal function.¹¹ In addition, the PLN-R14del mutation was associated with dramatically decreased cardiac contractile performance and increased susceptibility to triggered activity, both of which were reversed by the genetic correction that restored contractile function in hECT.¹²

In the present study, we fully characterized our recently developed knock-in mouse models expressing the human coding sequence of WT PLN (hPLN-WT) and/or mutant PLN (hPLN-R14del). Young adult (3- to 4-month-old) heterozygous hPLN-R14del mice with no overt cardiac microstructural or contractile abnormalities exhibited bi-ventricular dilation, increased stroke volume and protein alterations associated with

metabolic and contractile functional pathways. Furthermore, hPLN-R14del mice exhibited marked susceptibility to adrenergic-mediated VT, consistent with our recent studies.^{13,14} Our major focus here was to mitigate the observed abnormalities in cardiac function and arrhythmogenic susceptibility using the cardiotropic adeno-associated virus-9 (AAV9)-mediated approach to deliver gene-editing components. *In vivo* genome editing by AAV9-CRISPR/Cas9 successfully improved cardiac function and reduced arrhythmia vulnerability observed in *ex vivo* hPLN-R14del mouse hearts to WT levels. Further developed, these findings offer new insights that could translate to novel diagnostic and therapeutic strategies for patients with R14del mutation who currently have very limited medical treatment options.

2. Methods

An expanded methods section is provided in the [Supplementary material online](#).

2.1 Generation of humanized knock-in mouse model of PLN-R14del cardiomyopathy

Mice harbouring the human WT or mutant (R14del) coding sequence of PLN were generated by inserting *LoxP-H2B-GFP-4XpolyA-FRT-Neo-FRT-LoxP-hPLN^{WT/R14del}* cassette into the start codon at exon 2 of PLN through gene targeting^{13,14} (Figure 1A). Long range polymerase chain reaction (PCR) was performed to screen the targeted embryonic stem (ES) cells [R1 cells (129/Sv × 129/Sv-CP)F1] with two pairs of primers (P1/P2 and P3/P4) to detect recombination at 5' and 3' arms, respectively. DNA fragments of about 6 kb were amplified when homologous recombination occurred at the 5' and 3' ends, respectively (Figure 1B). Positive ES cells carrying the recombinant allele were injected into blastocysts of C57Bl/6J mice to generate chimeras. The *GFP-Neo* selection cassette was removed by breeding the animals with *Sox2-Cre* mice (Jackson Laboratory). The genotypes of the animals were confirmed by tail PCR and Sanger sequencing (Figure 1C and D).

hPLN-WT and hPLN-R14del mice were generated at the institutional Mouse Genetics and Gene Targeting Core at the Icahn School of Medicine at Mount Sinai (ISMMS). Three- to four-month-old female and male mice were used to characterize the phenotype. Two-month-old hPLN-R14del mice received AAV9/CRISPR-Cas9-gRNA vector via tail vein injection. Eight weeks after gene delivery, electrophysiological and molecular studies were performed.

For cardiac magnetic resonance imaging (CMRI) procedure, mice were weighed and anaesthetized with isoflurane 1–5% and maintained with a nosecone 1–3% anaesthesia for the prep and duration of scanning. Mice were euthanized by cervical dislocation with 5% isoflurane anaesthesia via a vaporizer. All animal procedures were approved by, and performed in accordance with, the Institutional Animal Care and Use Committee of the ISMMS. The investigation conforms to the *Guide for the Care and Use of Laboratory Animals*.¹⁵

2.2 Statistics

Shapiro–Wilk test¹⁶ was performed and the distribution of the data was found to be normal. We used two-tailed unpaired Student's *t*-test to determine the significance between two groups, and ordinary one-way ANOVA, followed by Tukey's multiple comparison test, to determine the significance between three groups, assuming significance at $P < 0.05$. VT thresholds are expressed as mean ± standard error of the mean.

Other values are expressed as the mean ± standard deviation. Each figure legend indicates the respective *n* values. The analysis was performed using Prism7 (GraphPad software).

3. Results

3.1 Humanized knock-in mouse model of PLN-R14del disease

To investigate the pathological effects of PLN-R14del mutation, we generated knock-in mouse models expressing the human coding sequence of either WT or mutated (R14del) PLN. We thus obtained hPLN-WT and hPLN-R14del heterozygous mice (Figure 1).

To examine whether R14del mutation-induced structural alterations in the heart, we performed histological analysis using haematoxylin and eosin (H&E) and Masson's trichrome staining on 3- to 4-month-old hPLN-WT and hPLN-R14del mice. While Masson's trichrome showed no evidence of fibrosis in mutant hearts (Figure 2A), H&E staining of short-axis heart sections revealed the appearance of dilation of both ventricles in hPLN-R14del compared to hPLN-WT (Figure 2B).

Detailed characterization using CMRI, performed on 3- to 4-month-old hPLN-WT and hPLN-R14del male and female mice, revealed significant changes in ventricular geometry in the hPLN-R14del group. Specifically, left ventricular end-diastolic volume was significantly elevated in the hPLN-R14del compared to hPLN-WT mice (Figure 2C, [Supplementary material online, Videos S1 and S2](#)). Dilation was also evident in the right ventricle with the end-diastolic volume of hPLN-R14del mice being significantly higher than hPLN-WTs (Figure 2C, [Supplementary material online, Videos S1 and S2](#)). hPLN-R14del animals compensated for the resulting elevated wall stress with significantly higher stroke volumes (right and left ventricular stroke volumes) per Starling's law of cardiac mechanics (Figure 2C). Despite bi-ventricular dilation in the hPLN-R14del animals, they exhibited evidence of functional compensation such that left ventricular ejection fraction was not different in hPLN-R14del ($81.1 \pm 4\%$) vs. hPLN-WT ($81.3 \pm 2.8\%$). Hypercontractility in the mid-left ventricular cavity was confirmed with higher midwall fractional shortening in hPLN-R14del ($66 \pm 5.3\%$) vs. hPLN-WT ($59 \pm 6.4\%$; $P = 0.068$) (Table 1). Taken together, these profiles suggest the 3- to 4-month-old hPLN-R14del animals represent a pre-symptomatic dilated cardiac phenotype with compensated pump function.

3.2 Electrophysiological challenge reveals an arrhythmogenic phenotype in hPLN-R14del hearts

As we had previously established in a separate cohort of mice,¹⁴ arrhythmia vulnerability in this model could be unmasked *ex vivo* using a combined isoproterenol and rapid pacing protocol. This protocol was designed to progressively push the murine heart rate to at least two-fold of its basal rate and mimic the heart rate response to strenuous exercise and adrenergic stimulation, which are the typical triggers that promote SCD in ACM patients.^{17,18} We compared the stimulus train frequency that was required for induction of sustained VT following isoproterenol infusion in each heart (defined as VT threshold). Based on VT threshold values, we compared the percentage of hearts that exhibited sustained VT at or below a pre-defined cut-off pacing frequency of 22.5 Hz. Shown in Figure 3A are typical responses of hPLN-WT (top) and hPLN-R14del (bottom) hearts that follow challenge with β -adrenergic stimulation and

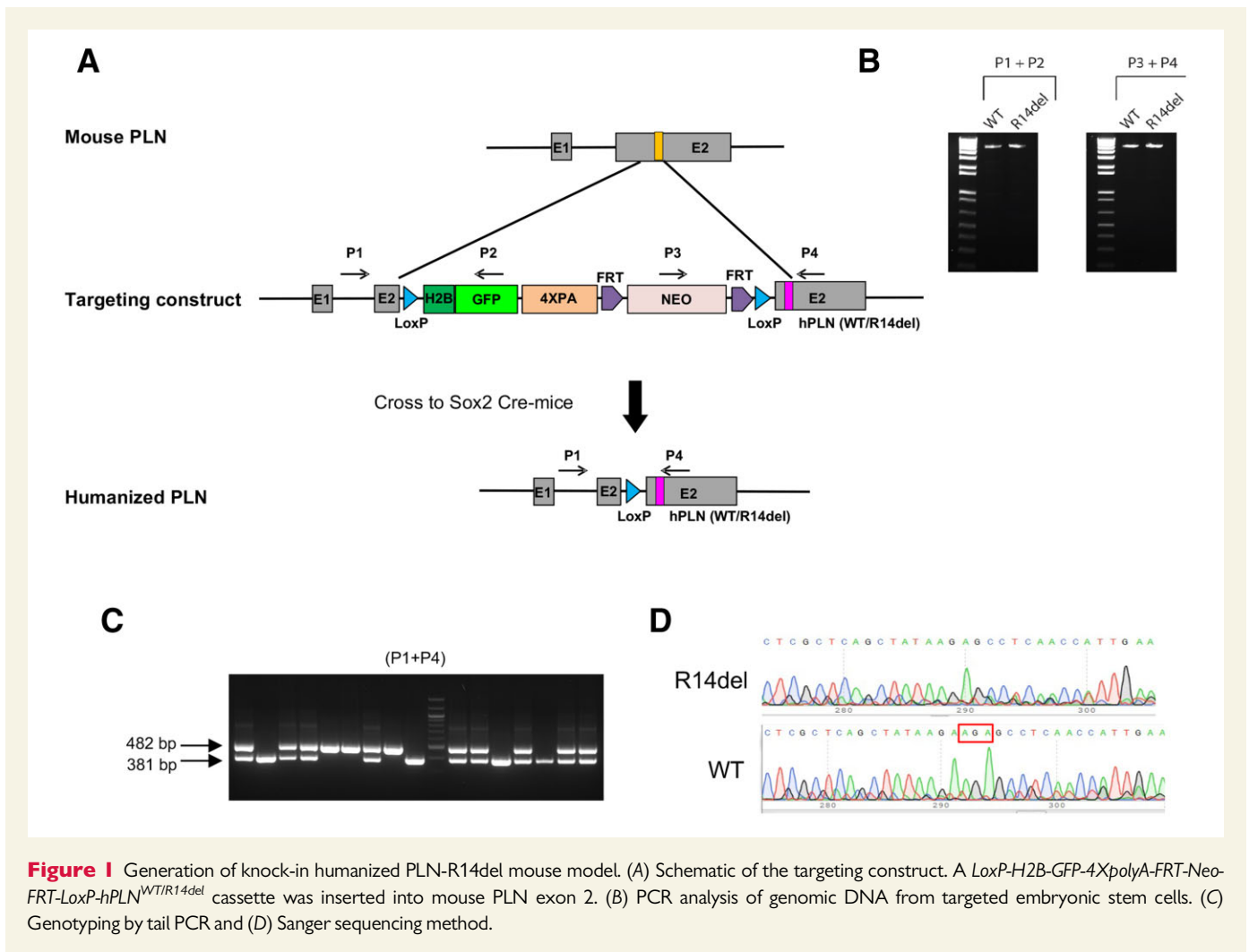


Figure 1 Generation of knock-in humanized PLN-R14del mouse model. (A) Schematic of the targeting construct. A *LoxP*-H2B-GFP-4XpolyA-FRT-Neo-FRT-LoxP-hPLN^{WT/R14del} cassette was inserted into mouse PLN exon 2. (B) PCR analysis of genomic DNA from targeted embryonic stem cells. (C) Genotyping by tail PCR and (D) Sanger sequencing method.

rapid pacing. The percentages of hearts that exhibited sustained VT at or below the pre-defined cut-off of 22.5 Hz (i.e. VT positive) vs. hearts that required faster pacing for VT induction (i.e. VT negative) were assessed in both groups (Figure 3B). At this cut-off, the majority of hPLN-R14del (75%, 6/8) but not hPLN-WT (27%, 3/11) hearts exhibited sustained VT. More importantly, quantification of VT threshold in all hearts from both groups regardless of cut-off is shown in Figure 3C. These data revealed significantly lower values in hPLN-R14del compared to hPLN-WT hearts, again consistent with significantly increased vulnerability to sustained adrenergic-mediated VT (hPLN-WT, 25.7 ± 1.3 Hz; hPLN-R14del, 20.3 ± 1.2 Hz, $P < 0.01$).

3.3 Proteomic analysis of right and left ventricles from hPLN-WT and hPLN-R14del mice

To characterize the molecular phenotype of PLN-R14del mice, we performed proteomic analysis of the right and left ventricles of 3- to 4-month-old hPLN-WT and hPLN-R14del mice (Figure 4A). Right and left ventricles displayed similar profiles of differentially expressed proteins, in terms of the numbers of up- and down-regulated proteins (Figure 4B). To further identify subcellular processes involved in PLN-R14del-induced cardiomyopathy, we subjected the differentially expressed proteins to dynamic enrichment analysis using the Molecular Biology of the

Cell Ontology (MBCO).¹⁹ Data from this analysis revealed up-regulation of a subset of proteins, in both right and left ventricles, associated with the glycolysis/glycogenolysis pathways, and down-regulation of mitochondrial proteins (Figure 4C).

In addition, proteins associated with myofilament formation, thin and thick myofilament organization, and Z-disk organization were increased in both right and left ventricles, indicating potential compensatory mechanisms in the remodelling phase of the hPLN-R14del hearts. Interestingly, we also observed an increase of desmosomal proteins in the left ventricle, which are known to be altered in ACM, a clinical phenotype associated with PLN-R14del patients.²⁰ Finally, the heat shock protein HSPD1, which is essential for the folding and assembly of newly imported proteins in the mitochondria, was decreased in the left ventricle of hPLN-R14del hearts (Figure 4C), suggesting an overall deficit in protein quality control, which would contribute to pathological alterations in the mutant hearts.

3.4 In vivo specificity of AAV9-CRISPR/SaCas9-gRNA_{R14del}

CRISPR/Cas9 is a powerful genome-editing tool,^{21,22} and AAV9-mediated delivery preferentially targets cardiac cells.^{23,24} Thus, we combined these two approaches as an exploratory, *in vivo* gene therapy strategy to target the disease phenotype associated with the

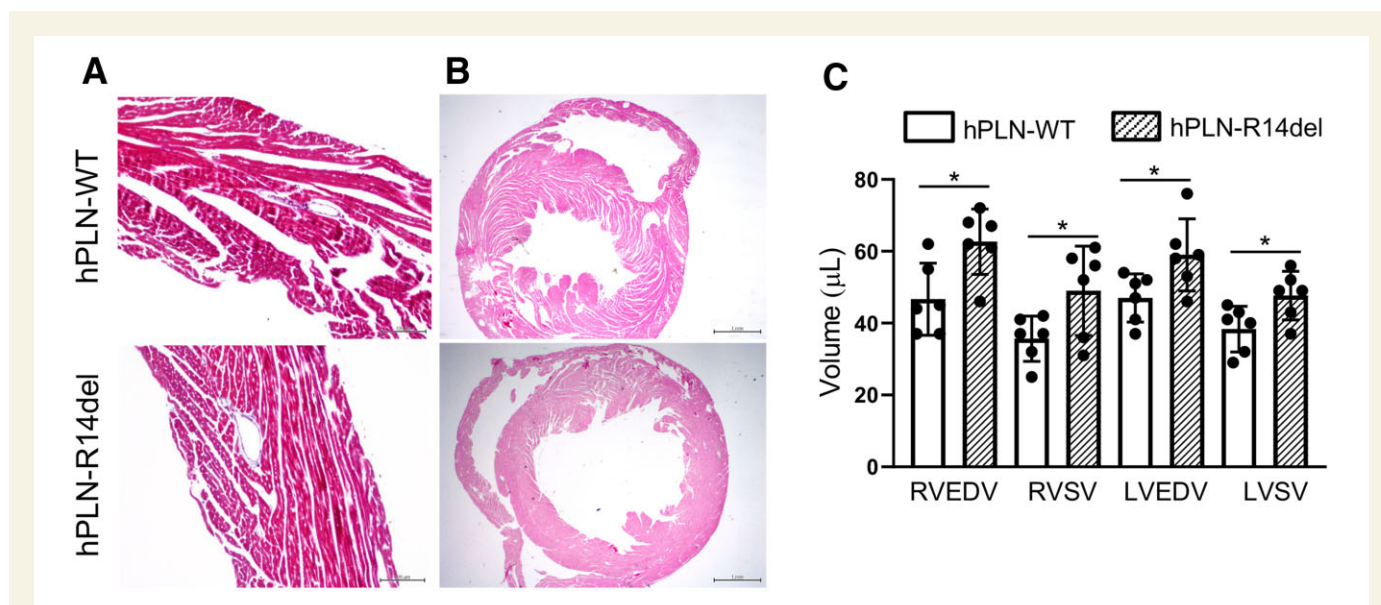


Figure 2 Histological analysis and cardiac MRI. Masson's trichrome (A) and haematoxylin and eosin (H&E) staining (B) of heart sections from hPLN-WT and hPLN-R14del mice. Scale bars, 100 μ m for panel A, 1 mm for panel B. (C) Bar graph showing right ventricular end-diastolic volume (RVEDV), left ventricular end-diastolic volume (LVEDV), and right and left ventricular stroke volume (RVSV and LVSV) measured by cardiac MRI ($n = 6$ per group; unpaired two-tailed Student's t -test. * $P < 0.05$).

Table 1 Cardiac magnetic resonance imaging parameters

	RVEDV	RVESV	RVS	RVEF%	LVEDD	LVESD	FS%	LVEDV
hPLN-WT	46.7 \pm 10.0	11.0 \pm 5.5	35.7 \pm 6.3	77 \pm 8.3	4.0 \pm 0.5	1.6 \pm 0.2	59 \pm 6.4	47 \pm 6.7
hPLN-R14del	62.7 \pm 9.1*	13.7 \pm 5.9	49 \pm 12.5*	77 \pm 11.3	4.3 \pm 0.3	1.5 \pm 0.2	66 \pm 5.3	62.5 \pm 8.1**
CRISPR-treated	45.4 \pm 4.2 [§]	13.0 \pm 3.4	33.6 \pm 3.4 [§]	74.0 \pm 3.5	4.0 \pm 0.3	1.9 \pm 0.3	54.1 \pm 5.6 [§]	51.4 \pm 5.2 [§]

	LVESV	LVS	LVEF%	LV mass	LV length	LV width
hPLN-WT	9 \pm 1.0	38 \pm 6.4	81.3 \pm 2.8	83 \pm 18.0	7.3 \pm 0.5	3.4 \pm 0.2
hPLN-R14del	11 \pm 4.3	49 \pm 4.4**	81.1 \pm 4.0	82 \pm 8.6	7.1 \pm 0.6	3.4 \pm 0.3
CRISPR-treated	13.2 \pm 2.6	38.6 \pm 4.2 [§]	74.6 \pm 4.5	75.6.0 \pm 9.9	7.4 \pm 0.2	3.6 \pm 0.4

Data are mean \pm SD (hPLN-WT, hPLN-R14del: $n = 6$; CRISPR-treated: $n = 5$; one-way ANOVA, Tukey's multiple comparison test.

* $P < 0.05$,

** $P < 0.01$ vs. hPLN-WT,

[§] $P < 0.05$ vs. hPLN-R14del).

FS, fractioning shortening; LVEDD, left ventricular end-diastolic diameter; LVEDV, left ventricular end-diastolic volume; LVESD, left ventricular end-systolic diameter; LVESV, left ventricular end-systolic volume; LVS, left ventricular stroke volume; RVEDV, right ventricular end-diastolic volume; RVEF, right ventricular ejection fraction; RVESV, right ventricular end-systolic volume; RVS, right ventricular stroke volume.

PLN-R14del mutation. We designed a CRISPR/Cas9-gRNA construct, which would cut around the site encoding the PLN-R14del gene. This would result in the introduction of indels by non-homologous end joining (NHEJ) and the subsequent inactivation of the gene. To check for CRISPR/Cas9 efficiency *in vivo*, we initially performed digital droplet PCR (ddPCR) using specific Genome Edit Detection assays, consisting of a primer pair to amplify the sequence that includes the mutation, and a FAM-labelled probe designed to specifically bind the mutant allele. A HEX-labelled reference probe distant from the nuclease target site was used to count the total number of genomes (Figure 5A). The FAM-labelled probe, which is specific for R14del mutation, should not bind

when the allele has an insertion or deletion (indels) at this site. The loss of FAM signal (while maintaining HEX signal) indicates the presence of an NHEJ allele. hPLN-WT mice were positive for HEX only, while the hPLN-R14del were positive for both HEX and FAM (Figure 5B), confirming the assay specificity. Six- to 8-week-old hPLN-R14del mice were next injected by tail vein with either 2×10^{12} vg AAV9.CRISPR/saCas9gRNA_{R14del} or the same dose of empty AAV9 particles as controls. Ventricular tissues or isolated cardiomyocytes were harvested when the mice reached the age at which we observed the disease phenotype (about 8 weeks post-treatment) and analysed for the presence of indels at on-target site in the genome. Digital droplet PCR analysis showed a

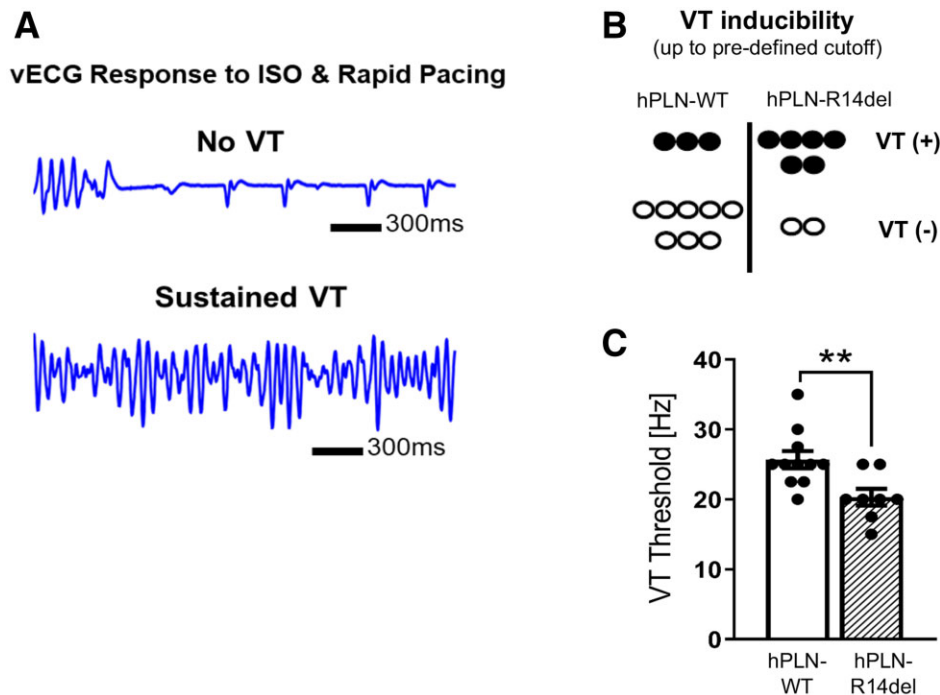


Figure 3 hPLN-R14del hearts showed increased risk of rapid pacing-induced arrhythmia. (A) Rapid pacing of isolated mouse hearts during adrenergic stimulation with isoproterenol (ISO) readily induced sustained ventricular tachycardia (VT) in hPLN-R14del group (bottom), whereas conversion to sinus rhythm was more prevalent in the hPLN-WT group (top), based on volumetric electrocardiogram (vECG) recordings. (B) the majority of hPLN-R14del (6/8) but not hPLN-WT (3/11) hearts exhibited sustained VT in response to challenge up to predefined cut-off frequency of 22.5 Hz. (C) A significant decrease in VT threshold was observed in the hPLN-R14del group compared to hPLN-WT (hPLN-WT: $n = 11$; hPLN-R14del: $n = 8$; unpaired two-tailed Student's t -test. $*P < 0.05$).

significant decrease of FAM signal ($10.2 \pm 3.4\%$ reduction, $P < 0.01$) in AAV9.CRISPR/saCas-gRNAR14del injected mice compared to controls, indicating the presence of indels at the R14del locus (Figure 5C). Of note, ddPCR showed a more pronounced decrease of FAM signal ($17.8 \pm 4.6\%$ reduction), when performed using genomic DNA extracted from isolated cardiomyocytes (Figure 5D), indicating that the percentage of edited DNA was diluted by non-cardiomyocytes in the ventricular tissues. As AAV9 shows levels of tropism towards the kidney and liver, we examined protein expression of SaCas9 in these organs. Data showed no presence of SaCas9 in the liver or kidney of CRISPR-treated mice (Supplementary material online, Figure S2D), whereas it was clearly expressed in $62 \pm 9.0\%$ ($P < 0.0001$) of nuclei within cardiomyocytes (Supplementary material online, Figure S3).

To precisely reveal the presence of indels at the Cas9-cleavage site, we used NGS-based amplicon sequencing approach in CRISPR-treated and control mice (Supplementary material online, Figure S4). Results showed equal abundance of mutant (R14del) and WT alleles in control hPLN-R14del mice (51.0% and 51.3% reads, respectively), whereas the mutant allele was less abundant than WT in CRISPR-treated hPLN-R14del mice (39% vs. 54% reads, respectively). In the CRISPR-treated hPLN-R14del mice, a remaining mean of 7% of total reads contained changes at the targeted genomic site including mostly deletions, leading to truncated PLN sequences.

We next determined the effect of DNA disruption on subsequent transcription and translation of PLN. *In vivo* genome editing induced allele-specific reduction of mutant PLN transcription with consequent

decrease of its translation (about 20%) as assessed by ddPCR and western blotting in CRISPR-treated hPLN-R14del mice compared to controls (Supplementary material online, Figure S5). Interestingly, NGS-based amplicon sequencing revealed that most indels were located at the Cas9-cleavage site and could produce frameshift mutations as revealed by the prevalent mutant sequences (Supplementary material online, Figure S3). No indels were present at the WT allele, indicating that gRNA can recognize a three-nucleotide difference and selectively target the R14del mutation in the mouse genome.

To evaluate the specificity of our gene editing approach, we analysed predicted off-target genomic sites for possible promiscuous editing. We have screened more than 5000 potential genome-wide off-target sites predicted by the COSMID design tool (<https://crispr.bme.gatech.edu>) by deep exome sequencing. By comparing the results between the control and treated samples, we found only one variant (G/A) as a possible off-target. This variant is in the non-coding region of chromosome 4 (position 43 510 088) of the mouse genome and, therefore, should not affect the protein-based sequence nor cardiac function.

3.5 CRISPR-Cas9-mediated genome editing partially rescues the disease phenotype observed in hPLN-R14del hearts

To evaluate the effect of CRISPR-Cas9 treatment on cardiac function, we performed magnetic resonance imaging in the hPLN-R14del

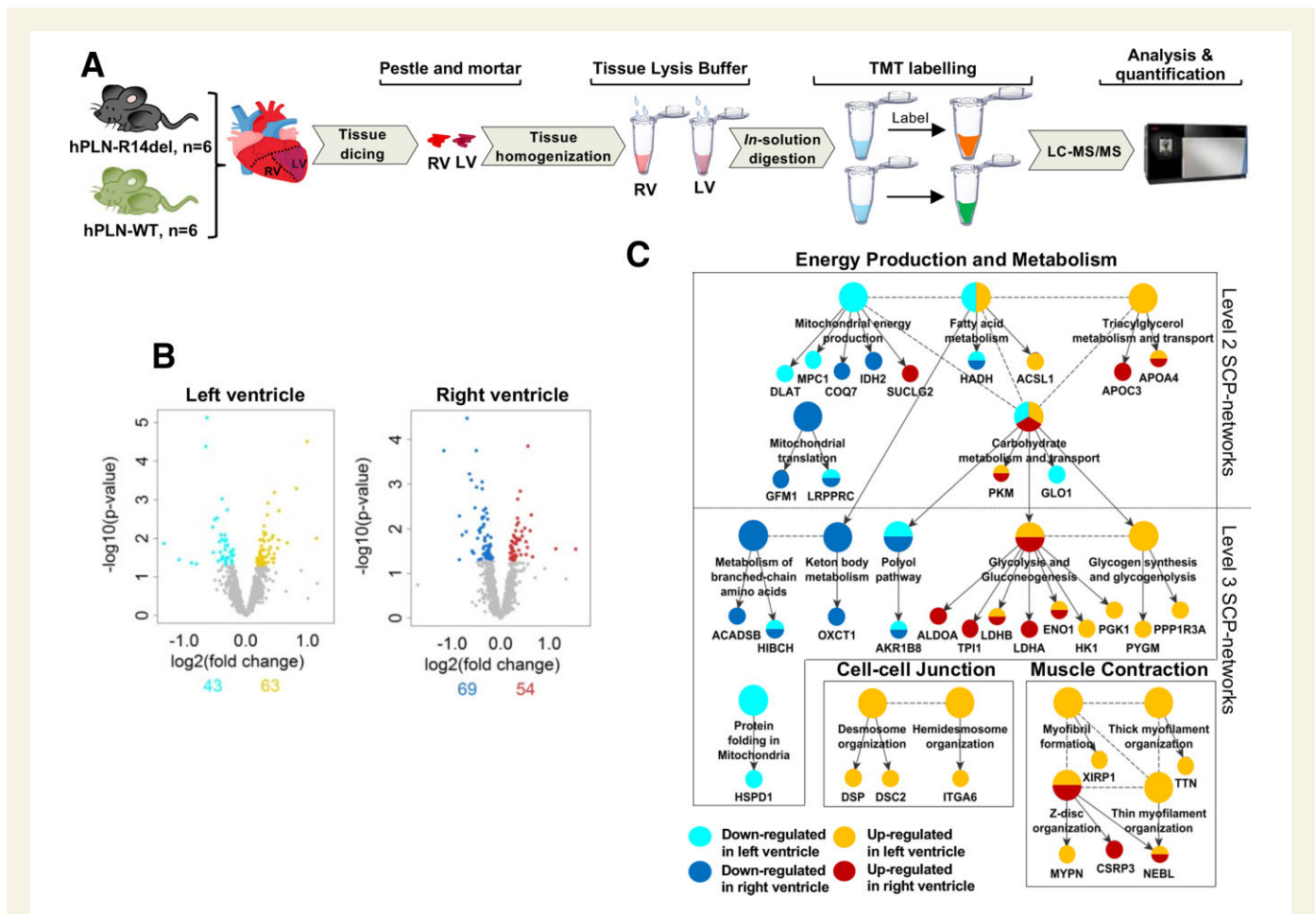


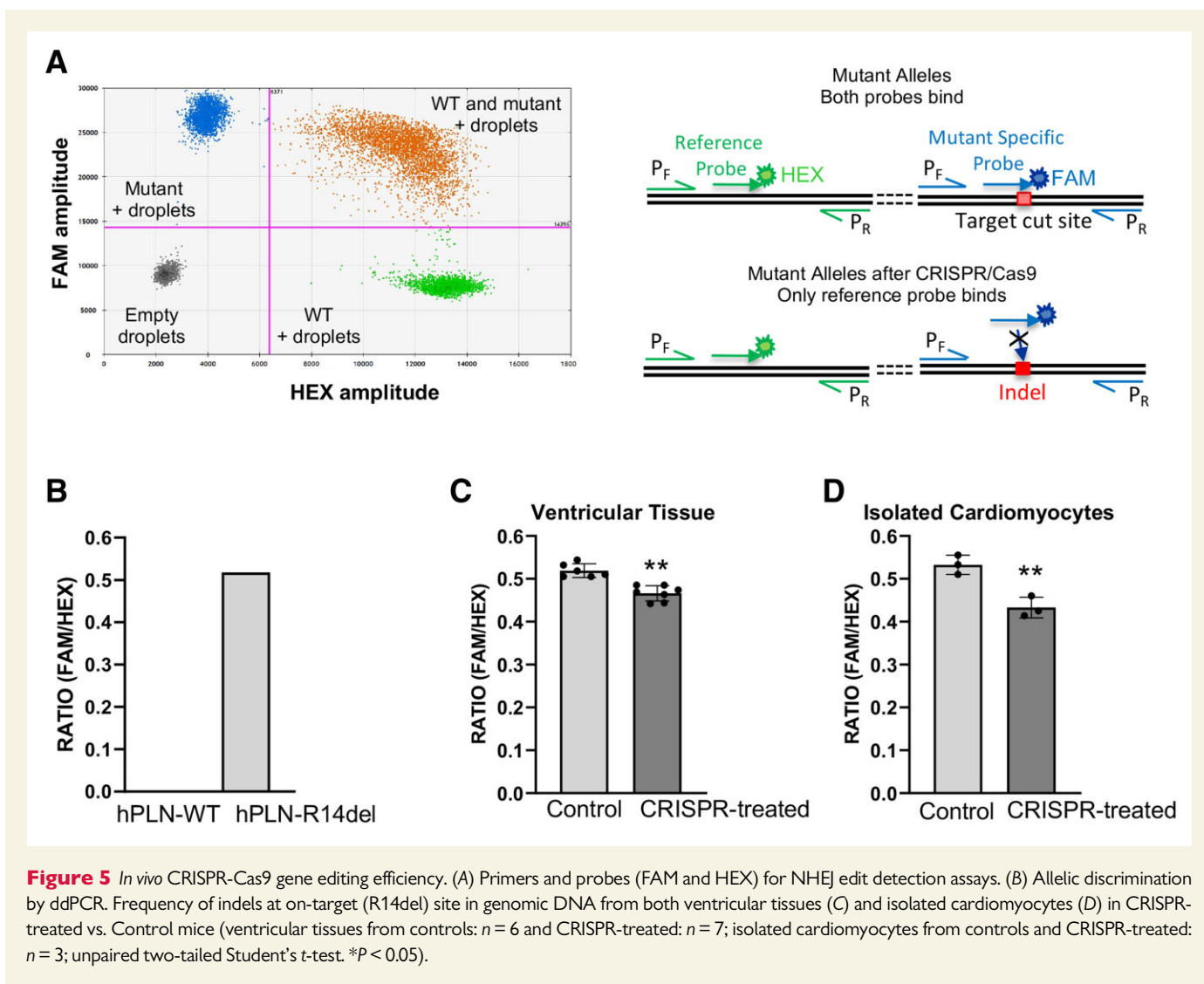
Figure 4 Proteomic analysis of right and left ventricles from hPLN-WT and hPLN-R14del mice. (A) Experimental design. (B) Volcano plots showing up-regulated (yellow, LV; red, RV) and down-regulated proteins (cyan, LV; dark blue, RV) in left ventricle (left panel) and right ventricle (right panel) based on proteomic analysis of the indicated samples ($n = 6$ per group). (C) Up- and down-regulated proteins in the left and right ventricle were subjected to dynamic enrichment analysis using the Molecular Biology of the Cell Ontology (MBCO), and disease relevant networks are shown. Arrows connect level-2 parent subcellular processes (SCPs) with their level-3 child SCs, and SCs with their annotated differentially expressed proteins. All proteins annotated to level-3 child SCs are also annotated to their level-2 parent SCs. For simplicity, we only show the annotation with level-3 child SCs in these cases. Dashed lines connect functionally related SCs of the same level, as predicted by the MBCO algorithm. Frames enclose SCP networks that converge on the indicated biological mechanism.

group, 8 weeks after treatment. As shown in Figure 6A and Table 1, CRISPR-treated mice showed significantly reduced right and left end-diastolic volumes and stroke volumes compared to hPLN-R14del mice treated with AAV9 empty capsids (controls), and they were not significantly different from hPLN-WT mice. We then evaluated the efficacy of CRISPR-Cas9 treatment in mitigating arrhythmia vulnerability. As Figure 6B shows, the percentage of ISO-treated hearts that exhibited sustained VT by the stimulus train at the pre-defined cut-off frequency was markedly lower in the CRISPR-treated group (12.5%, $n = 1/8$) compared to controls (66.7%, $n = 4/6$). The reduced proclivity for arrhythmia induction is further supported by the significant rise ($\sim 45\%$) in VT threshold in CRISPR-treated hPLN-R14del mice (30.9 ± 2.3 Hz) vs. controls (21.3 ± 1.5 Hz; $P < 0.01$, Figure 6C). Indeed, by adopting the same stress challenge protocol, we established that, in addition to a reduced VT susceptibility in the CRISPR-treated group, the pacing frequencies were more comparable to the ones observed in the hPLN-WT group (30.9 ± 2.3 vs. 25.7 ± 1.3 Hz, respectively).

4. Discussion

This study demonstrates a strategy to elicit evidence of impaired cardiac function and a heightened propensity for VT in seemingly asymptomatic hearts harbouring the human PLN-R14del mutation, and the ability to correct the disease phenotype *in vivo* by delivery of CRISPR/Cas9-gRNA using cardiotropic AAV9 gene transfer. We generated humanized mouse models in which only the coding sequence of mouse endogenous PLN gene was replaced by either the WT or mutant (R14del) human coding sequence of PLN.

CMRI revealed increases in right and left ventricular end-diastolic volumes (EDVs) without changes in systolic volumes. Interestingly, the hPLN-R14del mice exhibited no significant impairment in contractile function relative to hPLN-WT mice, as the ejection fraction was similar for both groups. In particular, the hPLN-R14del group exhibited significantly higher stroke volumes than hPLN-WT, primarily reflecting increased RV and left ventricular EDVs. *Ex vivo* studies revealed an



increased risk of sustained arrhythmia using a dual-hit protocol, where rapid pacing in the presence of beta-adrenergic stimulation unmasked heightened propensity to VT in the mutant group. Mice are important study tools to model human pathologies even though significant differences in cardiac physiology (and electrophysiology) exist between mice and humans. A mouse heart normally beats at a rate of about 10 Hz (i.e. up to 600 beats/min) which is 10-fold greater than that in humans. The mouse APD is about 25–30 ms (roughly 10-fold shorter than that in humans). Hence, adopting a challenge protocol that progressively pushes the murine heart rate above two-fold of its basal rate is a reasonable approximation of the heart rate response to strenuous exercise, which is a typical trigger that promotes SCD in ACM patients.²⁵

Using this protocol, we demonstrated that hPLN-R14del mice mimic the early stage (so-called concealed phase) of the disease phenotype that is characterized by a risk of arrhythmias that arise in the absence of overt heart remodelling in human carriers. Of note, the concealed phase of the disease is especially challenging because it often evades clinical detection by imaging modalities, including echocardiography and CMRI. Its pathophysiological significance, however, is clear considering that its first manifestation is often in the form of sudden cardiac death in young and seemingly healthy individuals.

The increased propensity to arrhythmia in our humanized mouse model was recently reported under pharmacological stress conditions *in vivo*.¹³ In addition, studies in isolated myocytes indicated that mutant RV myocytes exhibited depressed Ca^{2+} -cycling kinetics, prolonged action potential duration and increases in SR Ca^{2+} -leak and diastolic Ca^{2+} -levels. The number of aftercontractions upon stress conditions was also significantly higher in mutant RV cells. These RV-myocyte specific alterations resulted in *in vivo* arrhythmias under pharmacological stress conditions, that originated in the RV.¹³ Overall, our findings are compatible with the observations described in the clinical literature, where adrenergic-mediated mechanisms seem to be the culprit in triggering arrhythmias in heterozygous patients carrying the PLN-R14del mutation.¹

To further characterize the molecular phenotype of PLN-R14del mice, we performed proteomic analysis in the right and left ventricles of hPLN-R14del and hPLN-WT mice, which revealed: (i) activation of glycolysis/gluconeogenesis and glycogen synthesis/glycogenolysis pathways; (ii) inhibition of mitochondrial energy production; and (iii) up-regulation of muscle contraction and cell adhesion pathways. These findings suggest a remodelling of the metabolic network to favour a shift of substrate preference towards glucose, accompanied by an impaired myocardial energetic status and contractile dysfunction in hPLN-R14del hearts.

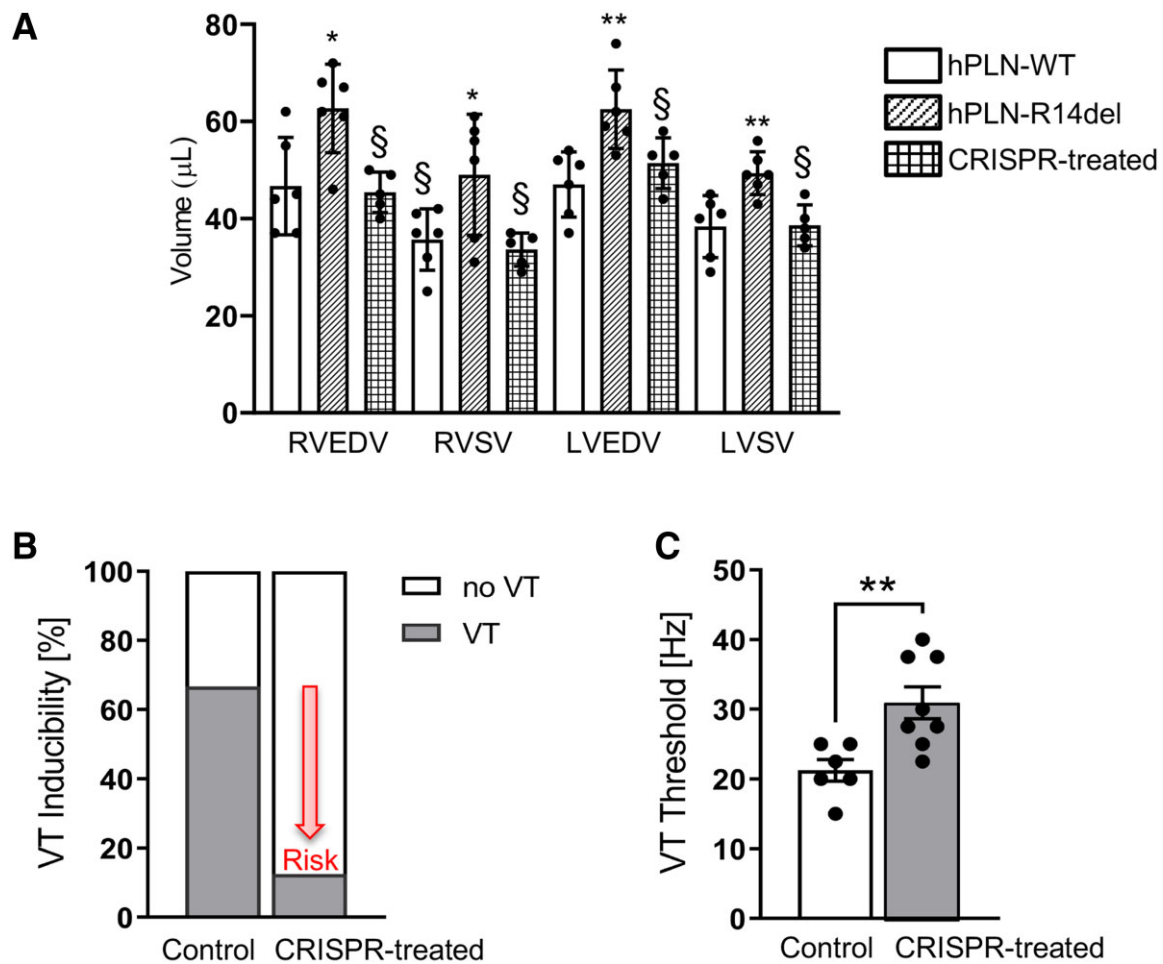


Figure 6 Effect of CRISPR treatment on cardiac function. CRISPR treatment significantly reduced ventricular end-diastolic and stroke volumes (A). (hPLN-WT: $n = 6$; hPLN-R14del: $n = 6$; CRISPR-treated: $n = 5$; one-way ANOVA, Tukey's multiple comparison test: $*P < 0.05$, $**P < 0.01$ vs. hPLN-WT, $§P < 0.05$ vs. hPLN-R14del). Greater than two-fold reduction of pacing induced arrhythmia by chosen cut-off of 22.5Hz (B) and a significant increase in VT threshold (C) revealed prominent decreased risk of pacing induced arrhythmia in the CRISPR-treated hPLN-R14del group (Controls: $n = 6$; CRISPR-treated: $n = 8$; unpaired two-tailed Student's t -test. $**P < 0.01$).

Overall, our data suggest that the right and left ventricles in hPLN-R14del hearts are adapting to adverse mechanical loads, with changes in electrophysiological characteristics associated with severe alterations in metabolic profiles.

We previously performed genome editing in patient-specific iPSC-derived cardiomyocytes and demonstrated that *in vitro* correction of R14del mutation could restore the aberrant Ca-cycling phenotype.¹¹ In that study, Transcription Activator-Like Effector Nucleases (TALEN) was used in the presence of a donor repair template to accurately correct the mutation through the precise homology-directed repair (HDR) mechanism. However, TALEN's cleavage efficiency is low, and HDR operates mainly in dividing cells and at very low frequencies in post-mitotic cells such as mature cardiomyocytes. Thus, in the present study, we developed a CRISPR/Cas9-based strategy to selectively target the mutant allele in heterozygous mice. CRISPR/Cas9 has higher expected cleavage efficiency than TALENs, and we designed gRNAs to specifically cut around the mutated site. *Staphylococcus aureus* Cas9-induced double-stranded DNA breaks are repaired by NHEJ (the most predominant cellular DNA repair pathway in non-dividing cells), which may lead to indels

at the targeted site. These indels frequently lead to a frameshift in the coding sequence, thereby disrupting gene expression. We successfully combined AAV9 and CRISPR/Cas9-gRNA gene-editing system to disrupt the PLN-R14del mutant allele in the mouse heart. Indeed, gene-editing induced deletion of base pairs at the target locus causing selective inactivation of the mutant allele while leaving the WT allele intact. Consequently, allele-specific CRISPR caused a reduction in mutant PLN transcript levels and subsequent decrease in PLN protein expression, likely due to a reduction of the mutated protein, thus preserving the WT PLN and its normal function.

These findings imply that a relatively low genome-editing efficiency was sufficient to improve the impaired cardiac function and the arrhythmogenic phenotype in the hPLN-R14del mice receiving AAV9-CRISPR/Cas9-gRNA injections. Of note, similar studies have suggested that small genome-editing efficiency is sufficient to produce significant therapeutic effects²⁶ or to induce a cardiac disease phenotype.²⁷ Interestingly, recent studies have also suggested that the correction of mutations within a small percentage of cells can improve muscle function.^{28,29} Further studies will be required to evaluate the potential for CRISPR/Cas9 gene

editing to improve the altered metabolic phenotype associated with the hPLN-R14del mutation.

4.1 Study limitations

This study has several limitations inherent to the use of mouse models, AAV vectors and genome editing. The mouse heart exhibits well-recognized species-specific differences compared to the human heart, including electrophysiology, myofilament protein composition, and Ca-cycling characteristics. Thus, mouse models do not typically recapitulate all aspects of human cardiovascular disease,³⁰ particularly in terms of heart rate and repolarization mechanisms. Therefore, extrapolation of the electrophysiological findings should be done with caution. Nevertheless, this proof-of-principle study showed that CRISPR/Cas9 could potentially alter the susceptibility to VT, the mechanism for which needs to be explored in future work. In relation to the therapeutic strategy, AAV vectors can last for a prolonged period of time (years in muscle),³¹ and continuous CRISPR/Cas9 activation may involve associated safety risks related to possible off-target effects. In this study, we screened more than 5000 potential genome-wide off-target sites by deep exome sequencing and found only one variant as a possible off target effect. Nevertheless, it will be important to further evaluate possible off-target effects of gene editing in longer-term studies. Long-term expression of Cas9 gene can also potentially trigger an immune response.³² Although a recent study that used CRISPR-Cas9 to correct muscular dystrophy has shown physiologic improvements up to 18 weeks post-treatment,³³ well beyond the window of an expected immune response, it remains necessary to assess immunogenicity in longer-term studies in order to advance *in vivo* gene therapy towards clinical trials.

5. Conclusions

In conclusion, we developed the first humanized knock-in mouse models (hPLN-WT and hPLN-R14del) designed for studying cardiomyopathies associated with PLN mutations. The mutant mice exhibited significant biventricular dilation with preserved ejection fraction, suggestive of a pre-symptomatic progression towards the DCM characteristic of PLN-R14del heterozygous patients. Interestingly, adrenergic stimulation combined with tachy-pacing unmasked an arrhythmogenic substrate in hearts from young mutant mice despite no clear evidence of structural or functional abnormalities such as fibrosis, fatty infiltrations, or contractile deficit. Since human PLN-R14del disease takes many years to manifest, often around the fourth decade of life, early detection of arrhythmia vulnerability could help identify carriers who are at risk of sudden cardiac death and might need stricter follow-up and targeted therapy, as supported by a previous report on Arrhythmogenic Right Ventricular Cardiomyopathy.¹⁷ Furthermore, CRISPR/Cas9-mediated gene editing *in vivo* in mutant mice successfully improved cardiac function and reduced VT susceptibility to WT levels, demonstrating tangible therapeutic benefits that offer new hope for treating patients with early stage PLN-R14del familial cardiomyopathy. More broadly, these findings support the concept that a CRISPR/Cas9-based strategy is valuable for further preclinical testing and represents an encouraging future therapy for patients with incurable monogenic disorders.

Supplementary material

Supplementary material is available at *Cardiovascular Research* online.

Authors' contributions

J.D. substantially contributed to the acquisition, analysis, and interpretation of data for the work, performed RNA, DNA and protein extractions, PCR and ddPCR analysis. N.R. performed Langendorff-perfusion and Arrhythmia induction experiments with the supervision of F.G.A. N.M. assisted in maintaining the mouse colony, performed genotyping, ddPCR, western blots, and immunofluorescence imaging. L.Z. and C.-L.C. designed the targeting strategy to generate the humanized knock-in mouse model. A.F. analysed MRI data. J.G.O. performed cardiomyocytes isolation, AAV tail injections, and assisted in maintaining the mouse colony. M.E.S. assisted in maintaining the mouse colony, performed western blots and genotyping. J.H. performed dynamic enrichment analysis of proteomic data. M.F., X.Y., and K.T. performed proteomic experiments and data analysis under the supervision of M.M. D.C. and M.N. designed guide RNAs and generated CRISPR-gRNA plasmids; D.C. also performed screening of guide RNAs. E.K., J.G.O., and L.W. generated AAV9-CRISPR/Cas9-gRNA. D.J. performed AAV tail injections and assisted in MRI data interpretation. J.D. and N.M. performed RNA, DNA and protein extractions, PCR and ddPCR analysis, N.M. also assisted in maintaining the mouse colony and performed immunofluorescence imaging. J.G.O. performed cardiomyocytes isolation, AAV tail injections, and assisted in maintaining the mouse colony. M.E.S. assisted in maintaining the mouse colony, performed western blot and genotyping. K.H. and I.C.T. reviewed the manuscript and made critical revisions. E.G.K. and K.D.C. assisted with interpretation of the findings, reviewed the manuscript, and made critical revisions. R.J.H. developed the concept, assisted with interpretation of the findings, reviewed the manuscript, and made critical revisions. F.S. substantially contributed to the conception and design of the work, supervised the experiments, interpreted data, and wrote the manuscript.

Acknowledgements

We thank the Mouse Genetics and Gene Targeting Core at ISMMS for microinjection of selected embryonic stem cell clones into mouse blastocysts to establish chimeric mice for the production of the knock-in mouse lines; the Biomedical Engineering and Imaging Institute at ISMMS for supporting the *in vivo* cardiac MRI; and Dr. Virginia Gillespie, DVM, of the Comparative Pathology Laboratory, Center for Comparative Medicine and Surgery at ISMMS, for providing a detailed morphologic description of H&E and trichrome stained sections of the examined hearts. Microscopy and/or image analysis was performed at the Microscopy CoRE at the Icahn School of Medicine at Mount Sinai.

Conflict of interest: K.D.C. discloses his role as scientific co-founder and Chief Scientific Officer of NovoHeart Ltd. NovoHeart did not play any role in the design or conduct of this study. E.G.K. is a scientific co-founder of Nanocor. Nanocor did not play any role in this study. The other authors declare that no conflicts of interest exist.

Funding

This work was supported by the American Heart Association [18TPA34230062 to F.S.], a grant from the Leducq Foundation [18CVD01 to E.G.K. and K.D.C.], and the National Institutes of Health [1R01HL131735 and 1R01HL137036 to C.L.C. and R01HL132226 to K.D.C.].

Data availability

The mass spectrometry proteomics data have been deposited to the ProteomeXchange Consortium via the PRIDE³⁴ partner repository with the dataset identifier PXD031612 and 10.6019/PXD031612". Reviewer account details: Username: reviewer_pxd031612@ebi.ac.uk; Password: Eu9gtspV.

References

- Haghighi K, Kolokathis F, Gramolini AO, Waggoner JR, Pater L, Lynch RA, Fan GC, Tsiapras D, Parekh RR, Dorn GW 2nd, MacLennan DH, Kremastinos DT, Kranias EG. A mutation in the human phospholamban gene, deleting arginine 14, results in lethal, hereditary cardiomyopathy. *Proc Natl Acad Sci USA* 2006;**103**:1388–1393.
- van der Zwaag PA, van Rijsingen IAW, Asimaki A, Jongbloed JDH, van Veldhuisen DJ, Wiesfeld ACP, Cox MGPJ, van Lochem LT, de Boer RA, Hofstra RMW, Christiaans I, van Spaendonck-Zwarts KY, Lekanne dit Deprez RH, Judge DP, Calkins H, Suurmeijer AJH, Hauer RNW, Saffitz JE, Wilde AAM, van den Berg MP, van Tintelen JP. Phospholamban R14del mutation in patients diagnosed with dilated cardiomyopathy or arrhythmogenic right ventricular cardiomyopathy: evidence supporting the concept of arrhythmogenic cardiomyopathy. *Eur J Heart Fail* 2012;**14**:1199–1207.
- van der Zwaag PA, van Rijsingen IAW, de Ruyter R, Nannenber EA, Groeneweg JA, Post JG, Hauer RNW, van Gelder IC, van den Berg MP, van der Harst P, Wilde AAM, van Tintelen JP. Recurrent and founder mutations in the Netherlands-Phospholamban p.Arg14del mutation causes arrhythmogenic cardiomyopathy. *Neth Heart J* 2013;**21**:286–293.
- Lopez-Ayala JM, Boven L, van den Wijngaard A, Penafiel-Verdu P, van Tintelen JP, Gimeno JR. Phospholamban p.arg14del mutation in a Spanish family with arrhythmogenic cardiomyopathy: evidence for a European founder mutation. *Rev Esp Cardiol (Engl Ed)* 2015;**68**:346–349.
- Posch MG, Perrot A, Geier C, Boldt LH, Schmidt G, Lehmkuhl HB, Hetzer R, Dietz R, Gutberlet M, Haverkamp VW, Ozcelik C. Genetic deletion of arginine 14 in phospholamban causes dilated cardiomyopathy with attenuated electrocardiographic R amplitudes. *Heart Rhythm* 2009;**6**:480–486.
- DeWitt MM, MacLeod HM, Soliven B, McNally EM. Phospholamban R14 deletion results in late-onset, mild, hereditary dilated cardiomyopathy. *J Am Coll Cardiol* 2006;**48**:1396–1398.
- Hof IE, van der Heijden JF, Kranias EG, Sanoudou D, de Boer RA, van Tintelen JP, van der Zwaag PA, Doevendans PA. Prevalence and cardiac phenotype of patients with a phospholamban mutation. *Neth Heart J* 2019;**27**:64–69.
- Te Rijdt WP, ten Sande JN, Gorter TM, van der Zwaag PA, van Rijsingen IA, Boekholdt SM, van Tintelen JP, van Haelst PL, Planken RN, de Boer RA, Suurmeijer AJH, van Veldhuisen DJ, Wilde AAM, Willems TP, van Dessel PFHM, van den Berg MP. Myocardial fibrosis as an early feature in phospholamban p.Arg14del mutation carriers: phenotypic insights from cardiovascular magnetic resonance imaging. *Eur Heart J Cardiovasc Imaging* 2019;**20**:92–100.
- van Rijsingen IA, van der Zwaag PA, Groeneweg JA, Nannenber EA, Jongbloed JD, Zwinderman AH, Pinto YM, Dit Deprez RH, Post JG, Tan HL, de Boer RA, Hauer RN, Christiaans I, van den Berg MP, van Tintelen JP, Wilde AA. Outcome in phospholamban R14del carriers: results of a large multicentre cohort study. *Circ Cardiovasc Genet* 2014;**7**:455–465.
- Haghighi K, Pritchard T, Bossuyt J, Waggoner JR, Yuan Q, Fan GC, Osinska H, Anjak A, Rubinstein J, Robbins J, Bers DM, Kranias EG. The human phospholamban Arg14-deletion mutant localizes to plasma membrane and interacts with the Na/K-ATPase. *J Mol Cell Cardiol* 2012;**52**:773–782.
- Karakikes I, Stillitano F, Nonnenmacher M, Tzimas C, Sanoudou D, Termglinchan V, Kong CW, Rushing S, Hansen J, Ceholski D, Kolokathis F, Kremastinos D, Katoulis A, Ren L, Cohen N, Gho J, Tsiapras D, Vink A, Wu JC, Asselbergs FW, Li RA, Hulot JS, Kranias EG, Hajjar RJ. Correction of human phospholamban R14del mutation associated with cardiomyopathy using targeted nucleases and combination therapy. *Nat Commun* 2015;**6**:6955.
- Stillitano F, Turnbull IC, Karakikes I, Nonnenmacher M, Backeris P, Hulot JS, Kranias EG, Hajjar RJ, Costa KD. Genomic correction of familial cardiomyopathy in human engineered cardiac tissues. *Eur Heart J* 2016;**37**:3282–3284.
- Haghighi K, Gardner G, Vafiadaki E, Kumar M, Green LC, Ma J, Crocker JS, Koch S, Arvanitis DA, Bidwell P, Rubinstein J, van de Leur R, Doevendans PA, Akar FG, Tranter M, Wang HS, Sadayappan S, DeMazumder D, Sanoudou D, Hajjar RJ, Stillitano F, Kranias EG. Impaired right ventricular calcium cycling is an early risk factor in r14del-phospholamban arrhythmias. *J Pers Med* 2021;**11**:502.
- Raad N, Bittihn P, Cacheux M, Jeong D, Ilkan Z, Ceholski D, Kohlbrenner E, Zhang L, Cai CL, Kranias EG, Hajjar RJ, Stillitano F, Akar FG. Arrhythmia mechanism and dynamics in a humanized mouse model of inherited cardiomyopathy due to phospholamban R14del mutation. *Circulation* 2021;**144**:441–454.
- Council NR. *Guide for the Care and Use of Laboratory Animals: Eighth Edition*. Washington, DC: The National Academies Press; 2011.
- Royston P. Approximating the Shapiro-Wilk W-test for non-normality. *Stat Comput* 1992;**2**:117–119.
- Denis A, Sacher F, Derval N, Lim HS, Cochet H, Shah AJ, Daly M, Pillois X, Ramoul K, Komatsu Y, Zemmoura A, Amraoui S, Ritter P, Ploux S, Bordachar P, Hocini M, Jaïs P, Haïssaguerre M. Diagnostic value of isoproterenol testing in arrhythmogenic right ventricular cardiomyopathy. *Circ Arrhythm Electrophysiol* 2014;**7**:590–597.
- Denis A, Sacher F, Derval N, Martin R, Lim HS, Pambrun T, Massoulié G, Duchateau J, Cochet H, Pillois X, Cheniti G, Frontera A, Takigawa M, Vlachos K, Martin C, Kitamura T, Hocini M, Douard H, Jaïs P, Haïssaguerre M. Arrhythmogenic response to isoproterenol testing vs. exercise testing in arrhythmogenic right ventricular cardiomyopathy patients. *Europace* 2018;**20**:f30–f36.
- Hansen J, Meretzky D, Woldesenbet S, Stolovitzky G, Iyengar R. A flexible ontology for inference of emergent whole cell function from relationships between subcellular processes. *Sci Rep* 2017;**7**:17689–17689.
- Rampazzo A, Calore M, van Hengel J, van Roy F. Intercalated discs and arrhythmogenic cardiomyopathy. *Circ Cardiovasc Genet* 2014;**7**:930–940.
- Wang H, Yang H, Shivalila CS, Dawlaty MM, Cheng AW, Zhang F, Jaenisch R. One-step generation of mice carrying mutations in multiple genes by CRISPR/Cas-mediated genome engineering. *Cell* 2013;**153**:910–918.
- Mali P, Yang L, Esvelt KM, Aach J, Guell M, DiCarlo JE, Norville JE, Church GM. RNA-guided human genome engineering via Cas9. *Science (New York, NY)* 2013;**339**:823–826.
- Bish LT, Morine K, Sleeper MM, Sanmiguel J, Wu D, Gao G, Wilson JM, Sweeney HL. Adeno-associated virus (AAV) serotype 9 provides global cardiac gene transfer superior to AAV1, AAV6, AAV7, and AAV8 in the mouse and rat. *Hum Gene Ther* 2008;**19**:1359–1368.
- Ishikawa K, Weber T, Hajjar RJ. Human cardiac gene therapy. *Circ Res* 2018;**123**:601–613.
- Zorzi A, Cipriani A, Bariani R, Pilichou K, Corrado D, Bauce B. Role of exercise as a modulating factor in arrhythmogenic cardiomyopathy. *Curr Cardiol Rep* 2021;**23**:57.
- Xie C, Zhang YP, Song L, Luo J, Qi W, Hu J, Lu D, Yang Z, Zhang J, Xiao J, Zhou B, Du JL, Jing N, Liu Y, Wang Y, Li BL, Song BL, Yan Y. Genome editing with CRISPR/Cas9 in postnatal mice corrects PRKAG2 cardiac syndrome. *Cell Res* 2016;**26**:1099–1111.
- Johansen AK, Molenaar B, Versteeg D, Leitoguinho AR, Demkes C, Spanjaard B, de Ruyter H, Akbari Moqadam F, Kooijman L, Zentilin L, Giacca M, van Rooij E. Postnatal cardiac gene editing using CRISPR/Cas9 with AAV9-mediated delivery of short guide RNAs results in mosaic gene disruption. *Circ Res* 2017;**121**:1168–1181.
- Long C, Amoasi L, Mireault AA, McAnally JR, Li H, Sanchez-Ortiz E, Bhattacharya S, Shelton JM, Bassel-Duby R, Olson EN. Postnatal genome editing partially restores dystrophin expression in a mouse model of muscular dystrophy. *Science* 2016;**351**:400–403.
- Nelson CE, Hakim CH, Ousterout DG, Thakore PI, Moreb EA, Castellanos Rivera RM, Madhavan S, Pan X, Ran FA, Yan WX, Asokan A, Zhang F, Duan D, Gersbach CA. *In vivo* genome editing improves muscle function in a mouse model of Duchenne muscular dystrophy. *Science* 2016;**351**:403–407.
- Milani-Nejad N, Janssen PM. Small and large animal models in cardiac contraction research: advantages and disadvantages. *Pharmacol Ther* 2014;**141**:235–249.
- Zacchigna S, Zentilin L, Giacca M. Adeno-associated virus vectors as therapeutic and investigational tools in the cardiovascular system. *Circ Res* 2014;**114**:1827–1846.
- Crudele JM, Chamberlain JS. Cas9 immunity creates challenges for CRISPR gene editing therapies. *Nat Commun* 2018;**9**:3497–3497.
- Bengtsson NE, Hall JK, Odom GL, Phelps MP, Andrus CR, Hawkins RD, Hauschka SD, Chamberlain JR, Chamberlain JS. Muscle-specific CRISPR/Cas9 dystrophin gene editing ameliorates pathophysiology in a mouse model for Duchenne muscular dystrophy. *Nat Commun* 2017;**8**:14454–14454.
- Perez-Riverol Y, Bai J, Bandla C, Garcia-Seisdedos D, Hewapathirana S, Kamatchinathan S, Kundu DJ, Prakash A, Frericks-Zipper A, Eisenacher M, Walzer M, Wang S, Brazma A, Vizcaino JA. The PRIDE database resources in 2022: a hub for mass spectrometry-based proteomics evidences. *Nucleic Acids Research* 2022;**50**:D543–D552.

Translational perspective

The phospholamban R14del mutation causes dilated and arrhythmogenic cardiomyopathies, with increased risk of malignant ventricular arrhythmias in young adult carriers. With few available therapeutic options, heart transplantation is often the ultimate treatment. This study reveals the ability to detect abnormal cardiac function and increased arrhythmogenic vulnerability in pre-symptomatic hPLN-R14del mice, and demonstrates that allele-specific disruption of R14del using *in vivo* AAV9/CRISPR-Cas9 reverses the disease phenotype. This preclinical study offers promising translatable approaches to detect and therapeutically suppress the arrhythmogenic phenotype in patients with PLN-R14del disease and potentially other inherited cardiomyopathies.